Science of the Total Environment 883 (2023) 163606

Contents lists available at ScienceDirect

Science of the Total Environment

journal homepage: www.elsevier.com/locate/scitotenv

Identification of pollutant delivery processes during different storm events and hydrological years in a semi-arid mountainous reservoir basin

Yan Jiang [a,b,*], Xin Bao [a,b], Zhengfang Huang [c], Yiping Chen [a,b], Xianing Wu [d], Xuyong Li [a,b], Xuefeng Wu [a,b], Yucong Hu [a,b]

[a] Research Center for Eco-Environmental Sciences, Chinese Academy of Sciences, Beijing 100085, China
[b] University of Chinese Academy of Sciences, Beijing 100049, China
[c] Beijing Hydrology Center, Beijing 100089, China
[d] PowerChina Resources Limited, Beijing 100044, China

HIGHLIGHTS

- N/P behaviors were analyzed during different storm events and hydrological years.
- Cumulative rainfall and runoff regime exerted significant control over N exports.
- Rainfall intensity and amount had significant control over P dynamics.
- Transmission pathways of TN were different in different hydrological years.
- TP were delivered mainly from overland sources by surface runoff.

GRAPHICAL ABSTRACT

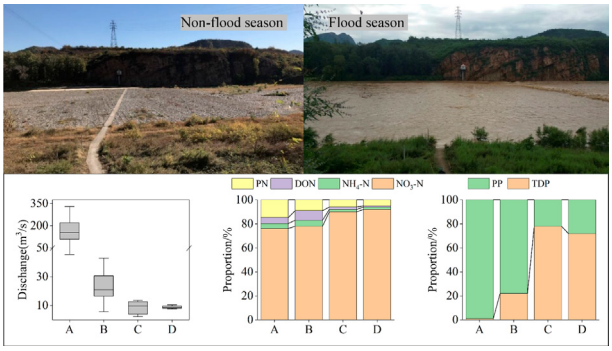

ARTICLE INFO

Editor: José Virgílio Cruz

Keywords:
Storm event
Nutrient dynamics
Hysteresis analysis
Hydrological years
Semi-arid mountainous reservoir basin

ABSTRACT

A comprehensive understanding of pollutant delivery processes during storm events is essential for developing strategies to minimize adverse impacts on receiving water bodies. In this paper, hysteresis analysis and principal component analysis were coupled with identified nutrient dynamics to determine different pollutant export forms and transport pathways and analyze the impact of precipitation characteristics and hydrological conditions on pollutant transport processes through continuous sampling between different storm events (4 events) and hydrological years (2018-wet, 2019-dry) in a semi-arid mountainous reservoir watershed. Results showed pollutant dominant forms and primary transport pathways were inconsistent between different storm events and hydrological years. Nitrogen (N) was mainly exported in the form of nitrate-N(NO_3-N). Particle phosphorous (PP) was the dominant P form in wet years, but total dissolved P (TDP) in dry year. Ammonia-N (NH_4-N), total P (TP), total dissolved P(TDP) and PP had prominent flushing responses to storm events and were delivered mainly from overland sources by surface runoff; while the concentrations of total N(TN) and nitrate-N (NO_3-N) were mainly diluted during storm events. Rainfall intensity and amount had significant control over P dynamics and extreme events played a key role in TP exports, accounting for >90 % of the total TP load exports. However, the cumulative rainfall and runoff regime during rainy season exerted significant control over N exports than individual rainfall features. In the dry year, NO_3-N and TN were delivered primarily through soil water flow paths during storm events; nevertheless, wet year registered complex control on TN exports via soil water release, followed by surface runoff transport. Relative to dry year, wet year registered higher N concentration and more N load exports. These findings could provide scientific basis for determining effective pollution mitigation strategies in Miyun Reservoir basin and provide important references for other semi-arid mountain watersheds.

* Corresponding author at: Research Center for Eco-Environmental Sciences, Chinese Academy of Sciences, Beijing 100085, China.
E-mail addresses: yanjiang@rcees.ac.cn (Y. Jiang), ychu2020_st@rcees.ac.cn (Y. Hu).

http://dx.doi.org/10.1016/j.scitotenv.2023.163606
Received 15 January 2023; Received in revised form 24 March 2023; Accepted 16 April 2023
Available online 25 April 2023

1. Introduction

The increasing nutrient inputs to surface water bodies can lead to water quality deterioration, such as eutrophication, high turbidity, water acidification and loss of biodiversity (Kelly et al., 2019). Researches demonstrated that nutrient inputs from several storm events could sufficiently represent the bulk of annual nutrient load to many rivers (Royer et al., 2006). Due to the differences of precipitation characteristics and watershed characteristics, nutrient compositions and their transport pathways are different in terms of mass and species distribution during the transformation through biological and physiochemical processes (Alvarez-Cobelas et al., 2008). Therefore, a better knowledge about how storm events mobilize nutrient, and how storm-mediated mobilization differs for nutrient are important for developing feasible pollution control strategies for highly impacted rivers and lakes (Pionke et al., 1999; Correll et al., 1999; Kelly et al., 2019).

Numerous studies have examined on nutrient dynamics during storm events in rivers, lakes, reservoir and wetlands (Quan and Meon, 2015; Adyel et al., 2017; Williams et al., 2018; Hinckley et al., 2019). Differences in nutrient export rates and discharge fluctuation rates during stormflow periods create precedes or lags in constituent concentration peak compared to the discharge peak. Thus, the hysteresis analysis for concentration-discharge relationship has been widely applied to assess pollutant sources and delivery pathways during storm events (Bowes et al., 2005; Lloyd et al., 2016; Aguilera and Melack, 2018; Williamson et al., 2020). The rainfall-runoff processes play a crucial role in biogeochemical cycles by delivering dissolved and particulate substances, mobilized over the soil surface and through soil layers, to river systems (Chen et al., 2012; Ma et al., 2016; Blaen et al., 2017; Nguyen et al., 2019). Therefore, stormflow and its runoff compositions are vital for nutrient export evaluations. Most of P in the soil exists attached to the soil particles; thus, soil erosion via surface runoff during storms is the main pathway of P export (Walling et al., 2003; Ballantine et al., 2006; Jarvie et al., 2012). But, dilution of P concentration was also noted to confirm that the subsurface runoff had more control over P exports (Burrus et al., 1990; Ballantine et al., 2008). Compared to P, NO_3-N and NH_4-N are highly mobile and easily leached within the soil and ended up in the groundwater primarily in the form of NO_3-N. Therefore, subsurface flow paths may be the dominant way of NO_3-N into the surface water bodies during stormflow periods (Pionke et al., 1999; Schilling and Zhang, 2004). However, some studies indicated that the total nitrogen and nitrate nitrogen mainly came from surface runoff (Owens et al., 2008). Janke et al. (2014) pointed out that the nutrient export pathway could change seasonally with the change of rainfall, production activities and other factors. These different views highlight the fact that the nutrient transport processes are far complex. Thus, further investigations are warranted.

The Chaohe river, located in the semi-arid region of North China, is an important upstream river affecting the water quality of Miyun Reservoir (Wang et al., 2018; Zhang et al., 2022). Miyun Reservoir is the only surface drinking water source of Beijing. To control waterbody pollution of the reservoir, a series of management policies have been issued for the upstream basin, such as establishing a national key prevention area for soil and water conservation (Zhao and Li, 1991), the Three-North Shelter Forest Project (Wang et al., 2010), the Beijing-Tianjin Sandstorm Source Control Project (Li et al., 2021), the Returning Farmland to Forest and Grassland Project, the Paddy Land-to-Dry Land Program (Zheng et al., 2013; Zhou et al., 2009), the application of soil testing and formulated fertilization technique (Cui et al., 2018), and so on. However, the water quality of Miyun Reservoir has not been significantly improved in recent decades. On the contrary, its nitrogen concentration fluctuated and increased, with an obvious eutrophication trend (Guo et al., 2021). One of the main reasons may be that storm event influences on water quality were ignored, and associated risks were underestimated.

Storm events establish strong hydrological links between overland pollutant sources and riverine regimes, and cause significant exports in nutrient and sediments particularly with diffused origin (Austin et al., 2004; Li et al., 2006). However, in semi-arid watersheds, most of the annual precipitation only occurs in the short rainy season and water quality monitoring has been confined to low resolution sampling (weekly or monthly). Storm event influences on water quality and associated nutrient loadings are less likely to be captured and underestimations on associated risks are possible. Thus, it is urgent to carry out hydrological and water quality monitoring of high-frequency to clarify how nutrients are transported from lands to rivers. However, the frequency that rainfall generates runoff is very limited (Jiang et al., 2015; Jiang et al., 2019). The uncertainty of whether rainfall produces runoff intensifies the complexity of nutrient export and migration (Mihiranga et al., 2021, 2022). At present, it is still unclear how rainfall characteristics affect the pollutant forms and transmission paths in semi-arid watersheds. Are there any other important factors affecting the pollutant delivery processes? Are the concentrations, loads and transmission paths of stormflow pollutant different in different hydrological years? Understanding the above problems will help for developing effective management strategies and providing a decision-making basis for water environmental treatments in the semi-arid mountainous reservoir watershed.

In this study, the components of N (NO_3-N, NH_4-N and TN) and P (TDP, PP and TP) were monitored by continuously sampling four storm events during rainy season in 2018 (a wet year) and 2019 (a dry year) in the Chaohe river basin. The key objectives of the study were: (1) to examine the effects of summer storms on N/P behavior traits; (2) to examine whether the delivery processes of N/P are different in different hydrological years.

2. Materials and methods

2.1. Study area

The Chaohe river is an inflow river of Miyun Reservoir in a semi-arid mountainous basin, with a drainage area of 5340 km^2 (Fig. 1) and a mean annual discharge of 82.3 $\times$ 10^8 m^3 (with ~75 % occurring in the wet season from June to September). The length of the main channel to the outlet is approximately 253 km and the river slope is 5.7 ‰. The climate type of this study area is the continental monsoon climate. The average annual temperature is 6–10 °C, with a maximum temperature of 37.8 °C and a minimum temperature of −28.6 °C. The average annual precipitation is 493 mm and the precipitation varies monthly and annually. Precipitation in flood season (June–September) generally accounts for 80 % of the annual precipitation, especially in July and August. The Chaohe river is a seasonal river, with groundwater buried about 30 m deep. The river is mainly recharged by precipitation, and the groundwater recharge is relatively small. Rainstorm is the dominant form of precipitation, with high rainfall intensity and strong erosivity, which provides power for the occurrence of non-point source pollution.

The topography in the Chaohe river watershed is mostly mountainous, with vertical zonality and abundant vegetation types. The vegetation is mainly composed of coniferous and broad-leaved mixed forests. The land use comprises 51.5 % forest, 36.8 % grassland, 10.5 % cultivated land, 1.8 % urban and residential land and 0.75 % villages. The most common soil types are brown soil and cinnamon soil, accounting for over 80 % of the total area. The Chaohe river basin covers four counties (Fengning, Luanping, Chengde, Xinglong and Miyun), with a total population of 365 thousand. Industrial point sources are better controlled in the watershed. Recent water quality degradation and eutrophication are mostly attributed to improper treatment of fertilizer application, livestock and poultry manure, domestic sewage discharge and soil loss.

2.2. Fieldwork arrangements and laboratory analysis

During the flood season in 2018 and 2019, the water quality and quantity were monitored synchronously in the lower reaches of the Chaohe river basin. Storm water was continually collected at the Xiahui hydrological station, the outlet of the Chaohe river (Fig. 1). The automatic rain gauge was installed at Xiahui Hydrological Station to collect real-time precipitation

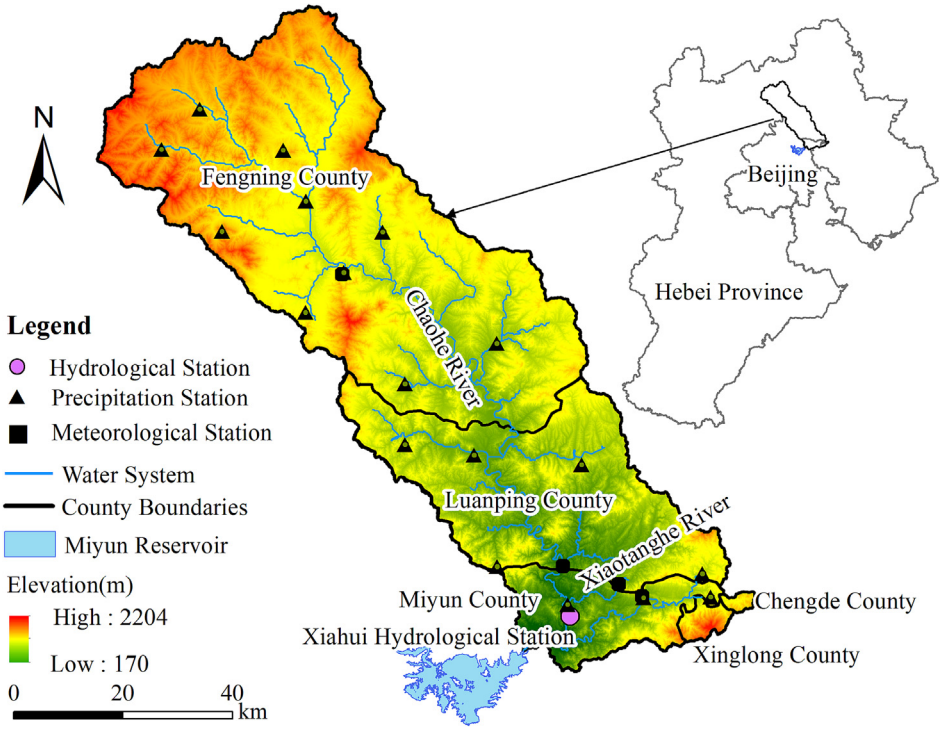

Fig. 1. Location of the study catchment and baseflow sampling locations.

data and the frequency was once a minute. Sampling was collected at intervals of 0.5–2 h when water level rises rapidly, and then 3–5 h' interval when water level recedes slowly to ensure that the sampling process covers the rising section, peak section and recession section of the flood process. We gathered the data of rainfall, discharge and nutrient concentration during storm events for analysis. The data sources of rainfall include the observation of automatic rain gauge set at the sampling point and the daily value data set of China surface climate data network. Instantaneous stream discharge during these storm events was measured by the staff at the Xiahui hydrological station through the velocity-area method.

The water samples were stored at 4 °C for laboratory analysis within 24 h. Stream discharge and water samples for chemical analysis were measured and collected manually at the Xiahui hydrometric station during four storm events. The samples were analyzed for these parameters: total nitrogen (TN), nitrate nitrogen (NO_3-N), ammonia nitrogen (NH_4-N), total phosphorous (TP), total dissolved phosphorous (TDP), particle phosphorous (PP) and total suspended solids (TSS). A portion of each water sample collected in the bottles was filtered (0.45 μm) and taken as the filtered sample, and the remainder was stored as the unfiltered sample. Filtered samples were analyzed for NO_3-N, NH_3-N and TDP, and the unfiltered water samples were analyzed for TN and TP. TN were determined using alkaline potassium persulfate digestion ultraviolet spectrophotometry (HJ636–2012); NO_3-N was determined using ultraviolet spectrophotometry (HJ/T346–2007); NH_4-N was determined N using Nessler's reagent spectrophotometry (HJ535–2009). TP and TDP were determined using ammonium molybdate spectrophotometry (GB11893–89). The determination method of each index conforms to the environmental protection industry standard of the People's Republic of China.

2.3. Data analysis

2.3.1. Event mean concentrations calculation

The event mean concentrations of pollutants (EMCs) are used to describe the impact of pollutant migration caused by rainfall on river water quality. Considering the pollutants from the point source emission and groundwater runoff, the relatively stable pollutant concentration of the river prior to a pulse on the hydrograph is taken as the baseflow concentration. The stormflow was defined as starting when discharged increased >20 %, and was considered to end when flow fell below 20 % compared to the previous baseflow (Kämäri et al., 2018). Then the stormflow load is total load minus baseflow load:

$$L = L_T - L_B \tag{1}$$

$$L_T = \sum_{i=1}^{i=n-1} \frac{c_i + c_{i+1}}{2} \times \frac{q_i + q_{i+1}}{2} \times \Delta t_i \tag{2}$$

$$L_B = c_B \times q_B \times \Delta t_i \tag{3}$$

$$Q = \sum_{i=1}^{i=n-1} \frac{q_i + q_{i+1}}{2} \times \Delta t_i \tag{4}$$

where, L is stormflow load (kg), L_T is total pollution load (kg), L_B is baseflow load (kg), and c_i is the concentration of pollutants at time step i (mg/l), q_i is the streamflow (m^3/s) at time step i, and Δt_i is the time interval between time step i and $i+1$ (s), c_B is the baseflow concentration (mg/l) before rainfall, q_B is the baseflow (m^3/s), and Q is the runoff (m^3). Therefore, the EMCs (mg/l) was calculated as:

$$EMCs = \frac{L_T}{Q} \tag{5}$$

2.3.2. Hysteresis analysis

Hysteresis can reflect concentration–discharge relationships and explain the source of pollutants. If there is a lag phenomenon between nutrient concentration and discharge, the change trajectory will form a circle graph which is called the hysteresis loop. Clockwise nutrient hysteresis patterns are generated when the concentration peak occurs on the rising stage of a hydrograph compared with the falling stage. Notably, an anti-clockwise hysteresis pattern means that the concentration peak appears later than the flow peak (Lloyd et al., 2016). A hysteresis index (*HI*) describes the degree of lag phenomenon. As the initial step,

instantaneous concentration and discharge measurements were normalized using the following equations:

$$Normalized\, q_i = \frac{q_i - q_{\min}}{q_{\max} - q_{\min}} \quad (6)$$

$$Normalized\, c_i = \frac{c_i - c_{\min}}{c_{\max} - c_{\min}} \quad (7)$$

Then the hysteresis index (*HI*) was calculated using:

$$HI(q_i) = c_{RL}(q_i) - c_{FL}(q_i) \quad (8)$$

$$HI = \frac{1}{n}\Sigma HI(q_i) \quad (9)$$

where $HI(q_i)$ is the index at percentile *i* of discharge, $c_{RL}(q_i)$ is the nutrient concentration on the rising limb at percentile *i* of discharge, $c_{FL}(q_i)$ is the nutrient concentration at the equivalent point in discharge on the falling limb. Hysteresis index occupies values between −1 and + 1; the magnitude of values represents the loop size and the strength of hysteresis. The sign of index indicates the direction of the hysteresis loop. The positive sign of *HI* value indicates that it is clockwise lag phenomenon and the pollutants mainly come from surface runoff; while the negative sign indicates that it is anti-clockwise lag phenomenon and the pollutants primarily come from sub-surface runoff. Nevertheless, in larger watersheds, hysteresis patterns might also imply the relative distance of pollutant sources to the discharge point. Thus, Clockwise loops could result from sources closer to the discharge point, while counter-clockwise loops might reflect distant pollutant sources.

2.3.3. Principal component analysis

Principal component analysis (PCA) was performed to identify the impacts of rainfall characteristics and discharge conditions on N/P dynamics during studied storm events of the dry and wet years. PCA analysis results are displayed in 2d scale and organized into the first and second principal components (PCs) which explain most of the variability with the data set. Variables which have higher correlation and interdependency are displayed closer together in the horizontal and vertical axis. The arrangement of variables along the horizontal axis is the most important.

2.3.4. Hierarchical partitioning analysis

The rainfall and discharge influencing factors are interdependent and interactive due to the complex rainfall-runoff mechanisms. Hierarchical partitioning analysis (HPA) was performed to explore the important impact factors on N/P dynamics (Zhang et al., 2020). The HPA was implemented in the R statistical package of "hier.part" (R Core Development Team, 2008), which can determine the key impact factors and effectively remove or weaken multicollinearity between influencing factors.

3. Results and analysis

3.1. Storms characteristics

Data for the four storm events on July 24, August 11 in 2018 and August 6, August 15 in 2019 were collected. Storm events were classified into different categories based on the total 24-hour rainfall amount; small storm: < 10 mm; moderate storm: 10–25 mm; large storm: 25–50 mm (storms B, C and D); extreme storm: >50 mm (storm A). According to the daily rainfall data of all precipitation stations in the Chaohe river basin from 1973 to 2020, the annual average rainfall was calculated and then the Pearson III frequency curve was plotted. The years with precipitation guarantee rates of 25 %, 50 %, and 75 % are respectively considered as wet years, normal years, and dry years. Among them, 2018 is a wet year and 2019 is a dry year. Table 1 presents the synthesized information on these events.

All four events showed the characteristics of typical short duration torrential precipitation in semi-arid mountainous areas. Storm A had the largest storm amount (127.6 mm), rainfall intensity (24.1 $mm{\cdot}h^{-1}$) and soil moisture (71 mm), which caused the largest flood process relative to other storm events. Peak discharge of storm A (330 $m^3{\cdot}s^{-1}$) at Xiahui hydrological station was 7.7, 24.6 and 31.4 times those of storms B (42.9 $m^3{\cdot}s^{-1}$), C (13.4 $m^3{\cdot}s^{-1}$) and D (10.5 $m^3{\cdot}s^{-1}$), respectively (Fig. S1). In terms of the ratio of maximum to minimum discharge, the hydrological fluctuations of storms A, B, C and D were 7.3, 7.8, 4.73 and 1.38, respectively. Storm A experienced the characteristics of "steep rise and steep fall", with short duration and drastic changes and the other three flood processes took a long time. While storms B, C and D had similar maximum rainfall intensity, storm D exhibited the characteristics with the total rainfall (29.6 mm) among which the peak discharge of storm D was relatively small and the variation of discharge was relatively stable. Storm B had a large average flow than Strom C, albeit storms B and C had similar rainfall characteristics. The streamflow peaks of these four storms lagged behind the maximum precipitation by around 12 h, 22 h, 43 h and 20 h, respectively, which represented the time for the water to flow from the land into the river channel from upstream to downriver. A quicker time to peak could be due to larger rainfall amount, intensity and antecedent soil moisture. The characteristics of the storm events presented here can be used for examining the storm effects on riverine N and P dynamics.

3.2. Nutrient dynamics during storm events

Different rainfall-runoff-pollution processes occurred due to different rainfall characteristics. The discharge and nutrient concentration during storm periods were plotted and visually examined for the presence of nutrient dynamics and their relations to hydrological conditions.

3.2.1. N concentration and load behaviors

Riverine concentrations and the associated behavior of different inorganic N forms were clearly distinctive during the storms. Fig. 2 shows that the proportion of NH_4-N was small, the proportion of NO_3-N was

Table 1
Characteristic of rainfall and discharge.

Storm events	A(extreme storm)	B(large storm)	C(large storm)	D(large storm)
Data	2018/7/24	2018/8/11	2019/8/8	2019/8/15
Average temperature (°C)	24.3	25.1	27.1	24.6
Rainfall duration (h)	24	37	32	7
Total rainfall (mm)	127.6	75.6	71.3	29.6
Maximum rainfall intensity ($mm{\cdot}h^{-1}$)	24.1	21.2	20	21.8
Average rainfall intensity ($mm{\cdot}h^{-1}$)	5.32	2.04	2.23	4.23
Stormflow duration (h)	37	137	157	85
Streamflow range ($m^3{\cdot}s^{-1}$)	45.4–330	7.74–42.9	2.22–13.4	7.61–10.5
Mean streamflow ($m^3{\cdot}s^{-1}$)	162.02	25.22	8.27	8.88
API[a] (mm)	71	20	15	17
Total samples	9	19	29	8

[a] Antecedent precipitation index (API) values can be used to represent antecedent soil moisture among pre-storm conditions. $API = \sum_{i=1}^{n} k^i \cdot Pi$, Where *Pi* are the precipitation depths (mm) $1, 2, \cdots, i\,(i = 12)$ days prior to the storm events and *k* is a constant defined as 0.85 (Chen et al., 2012).

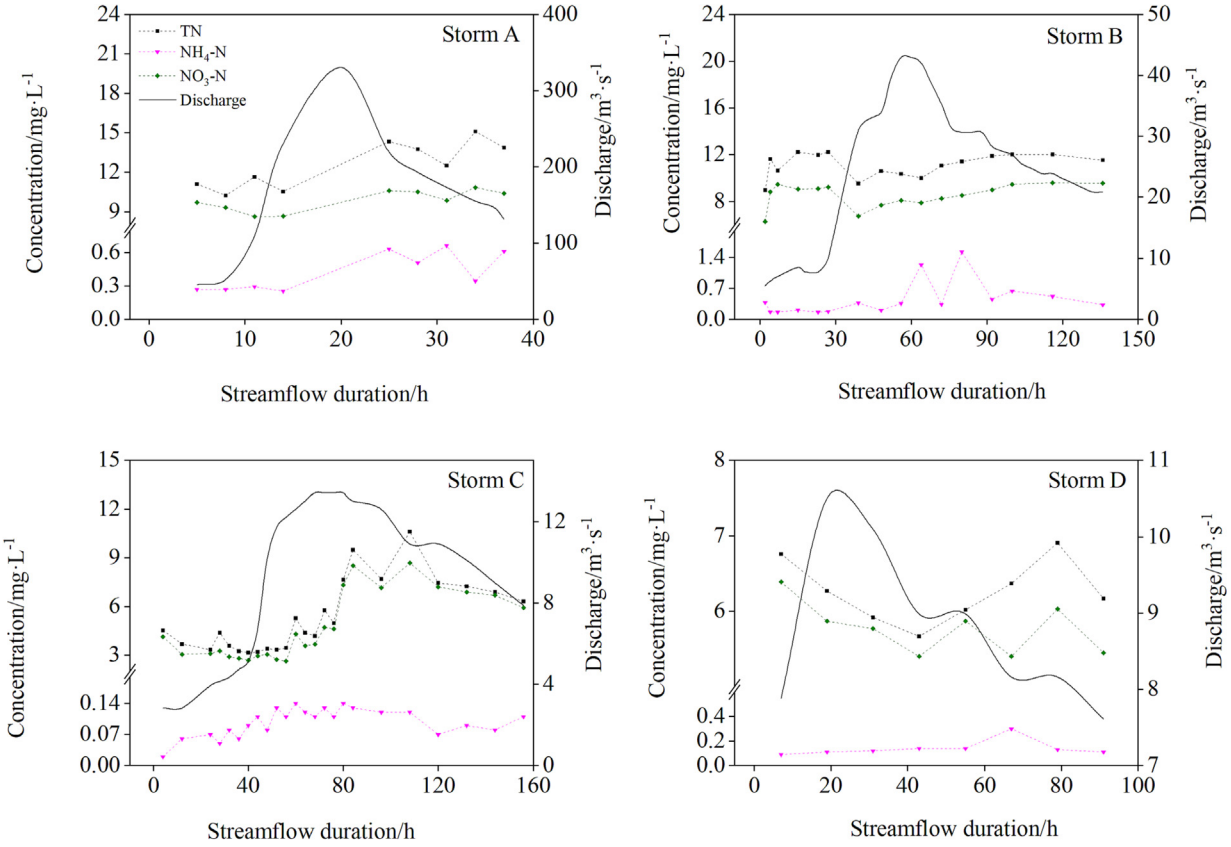

Fig. 2. Fluctuation of N concentrations and discharge during different storm events.

large, and the responses of different forms of N with flow fluctuation were different. The change process of NH_4-N concentration was similar to that of river streamflow. Nonetheless, NO_3-N concentrations were mostly diluted in response to discharge increments. Similarly, TN concentrations gradually declined to the bottom with the increase of runoff and showed a dilution pattern, and then rose with the decrease of runoff.

The variations of N concentrations and loads in the four storm events are shown in Table 2. The largest storm A registered the highest nitrogen concentration ranges, in which TN, NO_3-N and NH_4-N ranged 10.23–15.09 mg/L, 8.63–10.85 mg/L and 0.25–0.66 mg/L, respectively. The event-based ratios of maximum to minimum concentrations were smaller and nearly stable for TN (1.22–3.66) and NO_3-N (1.18–3.91) for different storm events. However, those of NH_4-N (2.6–8.90) were relatively wide and more variable between events. The event mean concentrations (EMCs) of different forms of nitrogen were the highest in the largest storm A, followed by storms B, C and D.

Table 2 indicates that NO_3-N was the dominant form of nitrogen export, accounting for 77–92 % of the total nitrogen export, while NH_4-N shared 2–5 % of TN load. Interestingly, NO_3-N in the smallest storm D contributed a large fraction of TN load (92 %) than that in storm A (77 %). The largest

Table 2
Summary of nitrogen concentrations and loads of four storm events and background flow nitrogen concentrations.

Feature	Event	TN	NO_3-N	NH_4-N	NO_3-N /TN	NH_4-N /TN
Pre-event concentrations	A	13.69	10.66	0.31	78 %	2 %
(mg/L)	B	8.97	6.31	0.39	70 %	4 %
	C	4.63	3.73	0.03	81 %	1 %
	D	6.76	6.39	0.09	95 %	1 %
Storm concentration	A	10.23–15.09	8.63–10.85	0.25–0.66	72 %–91 %	2 %–5 %
ranges (mg/L)	B	9.55–12.36	6.75–9.85	0.17–1.52	71 %–89 %	1 %–13 %
	C	2.9–10.62	2.22–8.68	0.02–0.14	74 %–97 %	0.4 %–4 %
	D	5.67–6.91	5.4–6.39	0.09–0.3	85 %–98 %	1 %–5 %
EMC (mg/L)	A	12.73	9.81	0.45	77 %	4 %
	B	11.3	8.84	0.56	78 %	5 %
	C	6.43	5.79	0.1	90 %	2 %
	D	6.22	5.75	0.15	92 %	2 %
Total loads (Ton)	A	274.73	211.71	9.71	77 %	4 %
	B	186.72	146.07	9.25	78 %	5 %
	C	37.52	33.79	0.58	90 %	2 %
	D	17.93	16.58	0.43	92 %	2 %
Stormflow load ratio[a]	A	77 %	77 %	84 %	–	–
	B	85 %	87 %	87 %	–	–
	C	78 %	88 %	91 %	–	–
	D	51 %	50 %	65 %	–	–

[a] Ratio of stormflow N load to total load (stormflow + subsurface stormflow).

storm A with the highest rainfall intensity registered the highest TN load exports (274.73 Ton), followed by storms B (186.72 Ton), C (37.52 Ton) and D (17.93 Ton). During storm periods, TN, NO_3-N and NH_4-N loads shared by stormflow were 51–85 %, 50–88 % and 65–91 % of the total loads (stormflow load + subsurface stormflow load) in storms A, B, C and D, respectively. It needed to point out that although the absence of water samples at the peak part of discharge may lead to some uncertainty of analysis, it did not affect the conclusion that the largest storm A registered the highest N concentrations and loads. In general, stormflow fluxes dominated the NH_4-N exports, while subsurface stormflow fluxes had more control over NO_3-N and TN exports.

3.2.2. P concentration and load behaviors

The dynamics of discharge and phosphorous (P) concentration during storm periods are displayed in Fig. 3. Apparently, riverine concentrations and the associated behavior of different P forms were distinctive during the storms. It can be seen from Fig. 3 that the proportion of particle phosphorous (PP) was large during storms A and B, but the proportion of the total dissolved phosphorous (TDP) was huge during storms C and D. In general, the change processes of TP, TDP and PP concentrations were similar to those of river streamflow. But the responses of different forms of P with flow fluctuation were different. In extrema storm A, the PP peak lagged behind the hydrograph peak during storm events. In storm B, PP had several peaks and the main peak (0.4 mg/L) lagged behind the first discharge peak for 8 h. In storm D, the TDP peak occurred simultaneously with the discharge peak, while it preceded the hydrograph peak during storm A and lagged behind the hydrograph peak during storms B and C.

The variations of phosphorous concentrations and loads in four storm events are shown in Table 3. The largest storm A registered the highest concentration ranges and EMCs of TP and PP. Among them, TP and PP ranged 0.33–7.8 mg/L and 0.28–7.74 mg/L; and EMCs of TP and PP were 4.18 mg/L and 4.12 mg/L, respectively. The EMC of TDP was the highest in storm C, followed by storms D, A, and B. In storm A, the EMCs were 4.06- and 4.25-times baseflow concentrations of TP and PP, respectively. During other storm events, the EMCs were lower than baseflow concentration for all different forms of phosphorous, indicating overall dilution of P concentration. The event-based ratios of maximum to minimum concentrations were greater and more variable for TP (2.1–23.8) and PP (3.5–27.8) over different storm events. Nevertheless, those of TDP (1.8–3.8) were relatively small and nearly stable between events.

It can be seen from Table 3 that PP was the dominant form of phosphorous export for storms A and B, accounting for 78–99 % of the total nitrogen export. For storms C and D, P was primarily exported as TDP, shared 72–78 % of TP load. The export mechanism of phosphorus was different for different rainfall intensity and rainfall amount. During storm periods, TP, PP and TDP loads shared by stormflow were 51–98 %, 48–98 % and 61–98 % of the total loads in storms A, B, C and D. In general, the dominant form of phosphorus export was inconsistent, which might be particle phosphorous or dissolved phosphorus during different storm events.

3.3. Transmission pathways of pollutants during storm events

Affected by watershed topography, vegetation cover, rainfall and other factors, there are great differences in transmission pathways of pollutants in different watersheds. A hysteresis analysis is an effective method to judge nutrient transmission pathways by analyzing the concentration–discharge patterns (Bowes et al., 2005; Chen et al., 2012). Concentrations of different water quality parameters produced different hysteresis loops trajectories during rising and falling limbs of hydrograph in different events.

3.3.1. Hysteresis behaviors and transmission pathways of N

To visually examine the presence of hysteresis effect, we plotted the concentration–discharge relationships of nitrogen throughout the four events (see Fig. 4). In all storm events, NO_3-N and TN produced counter-clockwise hysteresis with higher concentrations on the falling limb of the hydrographs, except for storm D. NH_4-N also displayed counter-clockwise hysteresis, except for storm C. Overall, NO_3-N dominated over TN hysteresis, and both recorded consistent hysteresis patterns through four storms. The largest negative *HIs* of NO_3-N (−0.80) NH_4-N (−0.64) and TN (−0.60) were recorded during storm A, which were associated with the largest event.

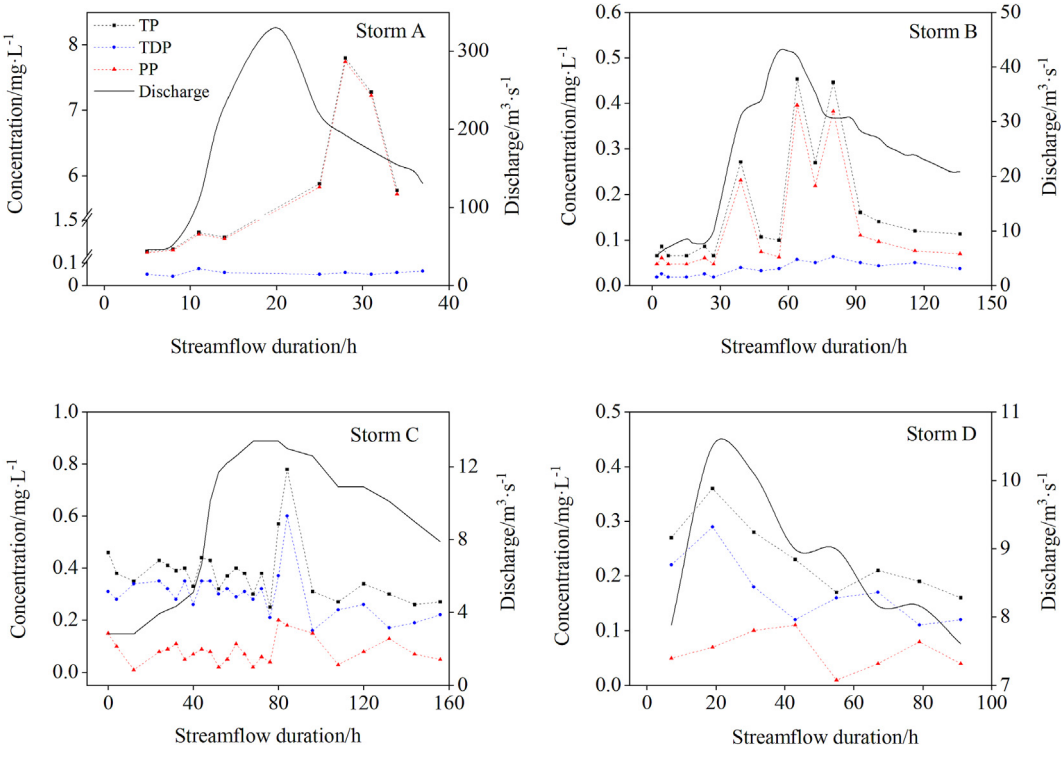

Fig. 3. Fluctuation of P concentrations and discharge during different storm events.

Table 3
Summary of phosphorous concentrations and loads of four storm events and background flow nitrogen concentrations.

Feature	Event	TP	TDP	PP	TDP /TP	PP/TP
Pre-event concentrations (mg/L)	A	1.03	0.06	0.97	6 %	94 %
	B	0.19	0.02	0.17	11 %	89 %
	C	0.46	0.31	0.11	67 %	33 %
	D	0.27	0.22	0.05	82 %	18 %
Storm concentration ranges (mg/L)	A	0.33–7.8	0.04–0.07	0.28–7.74	1 %–15 %	85 %–99 %
	B	0.07–0.45	0.02–0.06	0.05–0.39	13 %–43 %	57 %–87 %
	C	0.25–0.78	0.16–0.6	0.01–0.2	52 %–97 %	3 %–48 %
	D	0.17–0.36	0.11–0.29	0.01–0.11	52 %–94 %	6 %–48 %
EMC (mg/L)	A	4.18	0.06	4.12	1 %	99 %
	B	0.18	0.04	0.14	22 %	78 %
	C	0.36	0.28	0.08	78 %	22 %
	D	0.25	0.18	0.07	72 %	28 %
Total loads (Ton)	A	90.21	1.29	88.91	1 %	99 %
	B	2.97	0.66	2.31	22 %	78 %
	C	2.10	1.63	0.47	78 %	22 %
	D	0.72	0.52	0.20	72 %	28 %
Stormflow load ratio	A	94 %	78 %	94 %	–	–
	B	81 %	90 %	79 %	–	–
	C	98 %	98 %	98 %	–	–
	D	51 %	48 %	61 %	–	–

An anticlockwise hysteresis indicated soil water runoff was the main NO_3-N transport pathway, the nitrate could be replenished by delayed soil water runoff and had a longer flushing time. In storm D, NO_3-N demonstrated a clockwise trajectory, which means that the nitrate supply was primarily dominated by within-channel mobilization and diluted by increasing discharge. The dilution effect was mainly attributed to the dilution of solute in soil water by increasing discharge. In Chaohe river basin, agricultural fertilization is usually performed in spring and early summer. In summer rainy season, frequent rainfall flushing can alter the NO_3-N content in soil water, and the export of NO_3-N can gradually change from transportation restriction to source restriction. On the contrary, NH_4-N presented an anticlockwise trajectory. Its concentration increased with the increase of streamflow and reached a peak value at the descending section of the hydrograph, and then dropped to the previous concentration, indicating that the potential source of NH_4-N is far away from the monitoring point. In addition, most of NH_4-N was washed by surface runoff from the

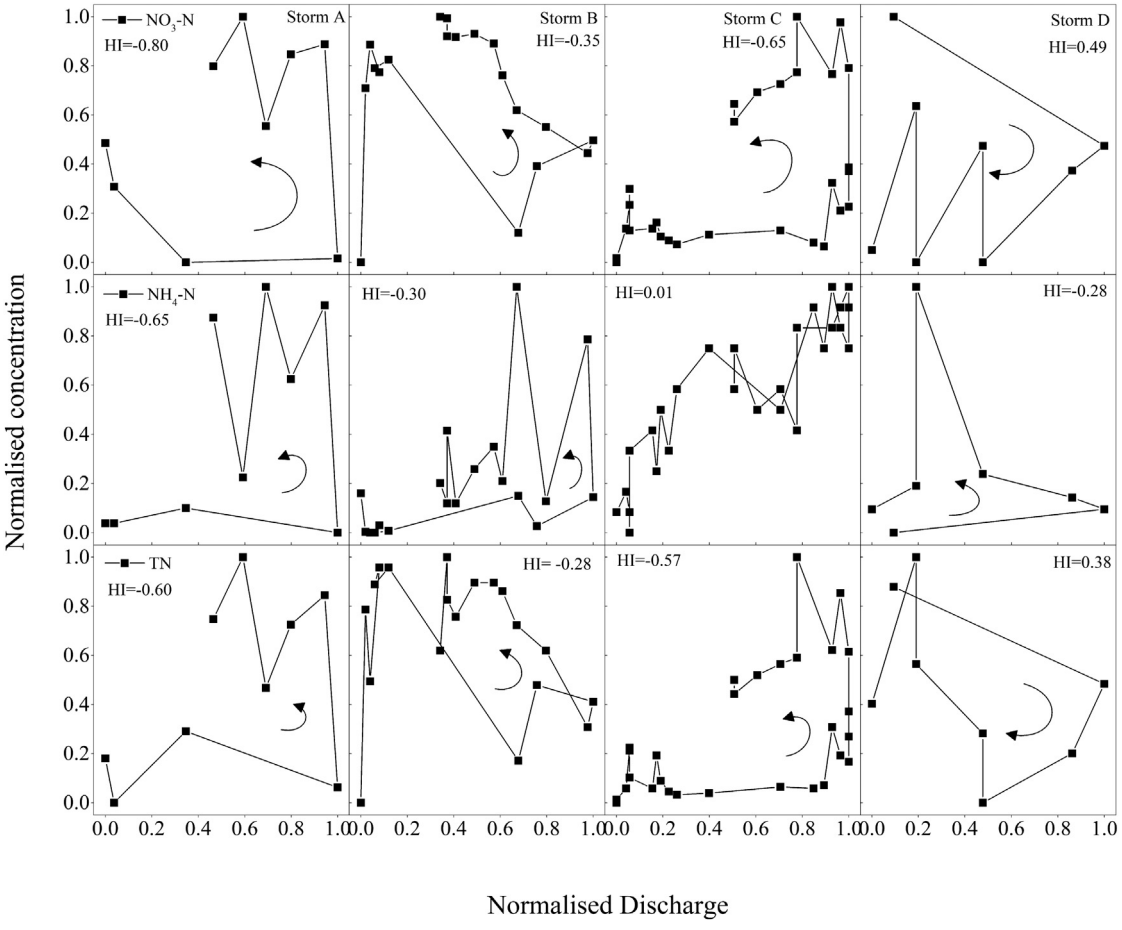

Fig. 4. Hysteresis patterns of N concentrations and discharge during different events.

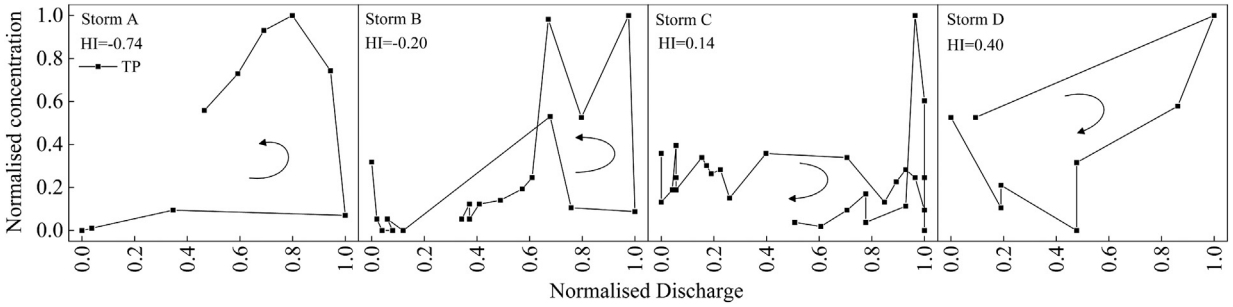

Fig. 5. Hysteresis patterns of TP concentration and discharge during different events.

upstream area and delayed to be transported downstream to the outlet. TN hysteresis behavior was consistent with NO_3-N during storms which indicated again that NO_3-N was the dominant form of nitrogen export and soil water runoff was the main hydrological pathway of TN export. Therefore, N management would require the reduction of nitrogen sources and the prevention of soil water pollution through infiltration by improving land management.

3.3.2. Hysteresis behaviors and transmission pathways of P

Fig. 5 showed the concentration–discharge relationships of TP throughout the four events. During storms A and B, TP produced counter-clockwise hysteresis with higher concentrations on the falling limb of the hydrographs, whereas displayed clockwise hysteresis during storm D. The largest HI of TP (0.74) were also recorded during storm A. In storms A and B, particle P was the dominant form of P export. PP was consistent with the increase of discharge and suspended sediment concentration (Figs. 3 and S3). This showed the removal of P from the cultivated area mainly in the form of particles. The migration of sediment and other particles caused by soil erosion lagged behind the runoff, resulting in the peak concentration of some pollutants adsorbed on sediment to lag behind the peak flow. The source of P pollutants in storms A and B mainly originated from surface sediments. In storms C and D, TDP was the dominant form of P export. The clockwise hysteresis indicated that TDP and TP delivered via surface runoff. In general, no matter the P export form was PP or TDP, the TP was transmitted through surface runoff.

3.4. Influencing factors of riverine nutrient

Rainfall drives the nutrient from basins to water body through runoff, soil erosion and farmland drainage (Alvarez-Cobelas et al., 2008). Due to different nutrient sources and rainfall characteristics, transmission pathways via storm runoff become complicated. Therefore, Principal Component Analysis (PCA) and Hierarchical Partitioning Analysis (HPA) were applied to determine the effects of rainfall, streamflow and antecedent soil moisture on N and P dynamics during storms (Figs. 6–7). Apparently, PC1 and PC2 explained over 90 % of the variation of the variables.

As shown in Fig. 6a, the concentrations and loads of all N variables were highly correlated with rainfall amount, intensity and mean streamflow in storms A and B. Compared with storms C and D, storms A (extreme) and B (large) contributed significantly to the N dynamics. And the HPA results revealed that mean discharge had a higher impact on the concentrations and loads of all N variables than precipitation factors, reaching over 50 % (Fig. 7a). Therefore, the N export processes were affected by the whole rainfall-runoff processes.

Fig. 6b showed that the concentrations and loads of all P variables (excluding TDP) correlated strongly with rainfall characteristics in storm A.

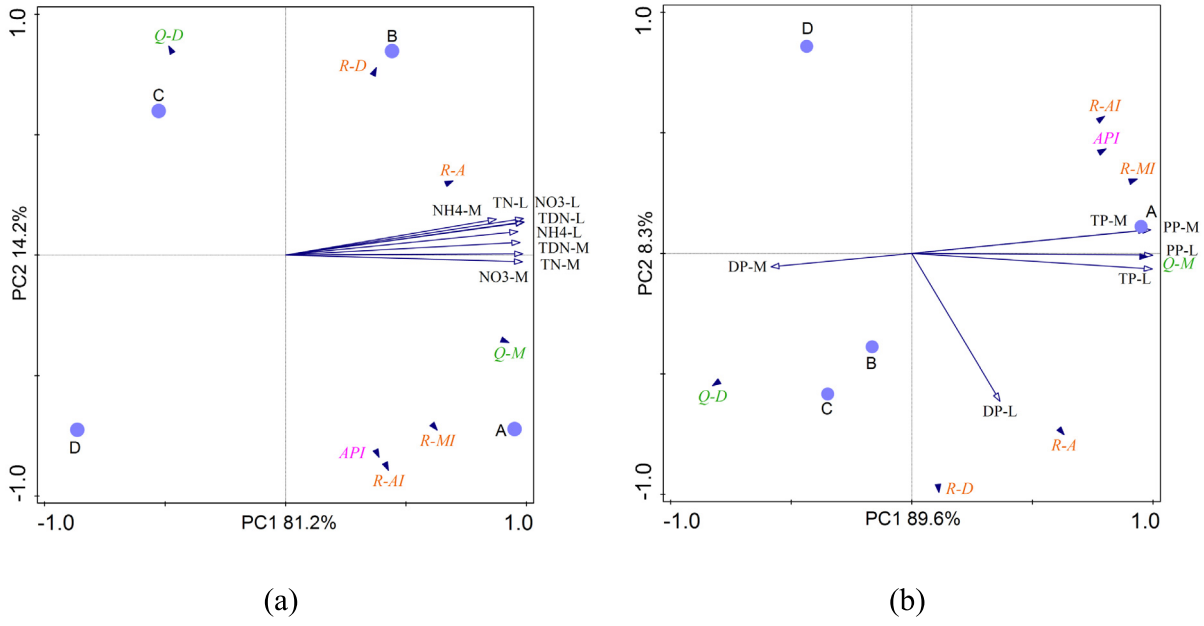

Fig. 6. Principal component analysis correlation among N(a)/P(b) variables, rainfall and discharge characteristics and antecedent soil moisture during storm events; A, B, C, D denotes four storms; Q-M and Q-D are mean discharge and stormflow duration, respectively; R-A, R-D, R-AI, R-MI, and API are rainfall amount, duration, average intensity, maximum intensity, and antecedent precipitation index, respectively; TN-L, TP-L, … are the respective N/P loads, while TN-M, TP-M, … are the respective N/P mean concentrations (i.e. EMCs).

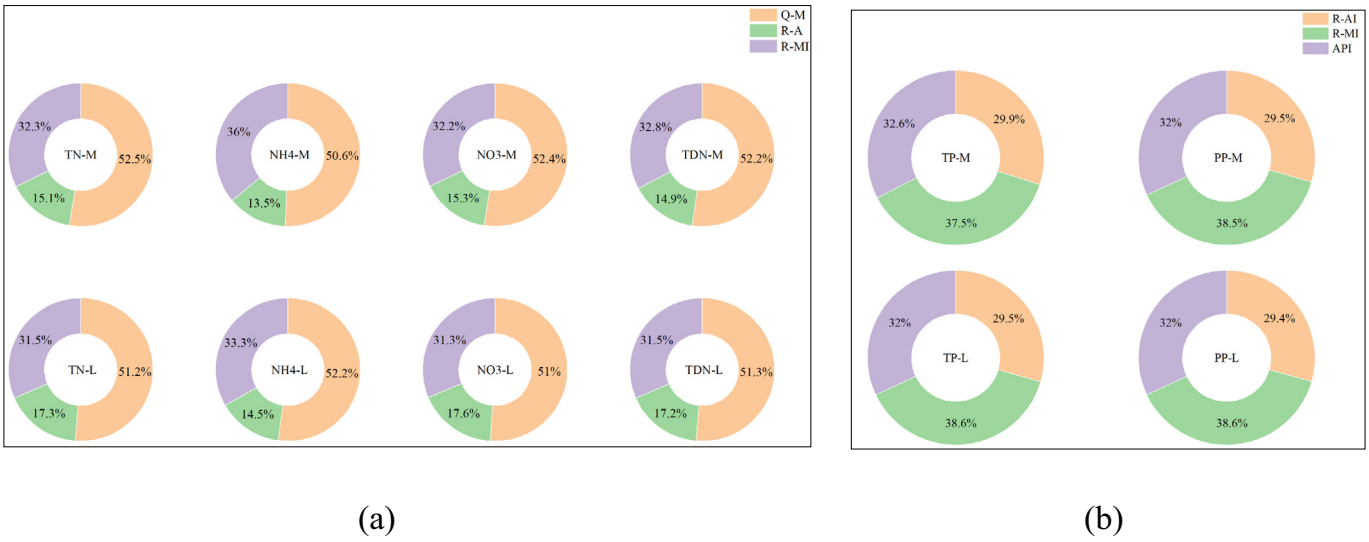

Fig. 7. The results of hierarchical partitioning analysis for N(a)/P(b).

The extreme storms determined the P load and concentration behaviors indicating influences of intensive rainfall on soil erosions and subsequent P exports. The HPA results indicated that the maximum precipitation intensity has the greatest impact on the concentrations and loads of P variables, followed by the average precipitation intensity and antecedent precipitation index (Fig. 7b).

4. Discussion

4.1. Effects of rainfall characteristics on nutrient transport processes

Basically, the nutrient export processes vary with rainfall intensity and amount (Wagne et al., 2008; Macrae et al., 2010; Chen et al., 2012; Bowes et al., 2015; Bender et al., 2018). However, it is still unclear how rainfall intensity, amount and duration affect pollutants transmission paths in semi-arid catchments. In this study, different pollutant export forms and transport pathways were studied in four storm events (including one extreme storm, three large storms) during rainy seasons of the Chaohe river basin.

Different rainfall events and associated hydrological conditions led to contrasting nutrient behavior responses between events and between components (Figs. 2-3, S2 and Tables 2-3). The extreme storm A experienced the highest mean concentration, concentration ranges and load exports for all N components, which meant the extreme storm with highest rainfall intensity and amount, mobilized significant amount of nutrient from board watershed regions to the near-stream regions. In the all four storms, the results of dilution of concentrations confirmed that the subsurface runoff had more control over NO_3-N and TN exports (Fig. 4). Surface stormflow fluxes still dominated NH_4-N exports.

Compared with nitrogen, the main composition and hydrological pathways of phosphorous exports were relatively complex. Rainfall amount and intensity had significant control over TP ($p < 0.05$). The PCA and HPA results (Fig. 6b and Fig. 7b) confirmed the correlations between P variables and rainfall characteristics in storm A. Extreme storm events played a vital role in P exports. In the extreme storm A, all P components had the highest mean concentration, concentration ranges, load exports and stormflow load ratio. The large storm A shared 94 % of total P exports. PP fractions increased markedly to 99 %, almost becoming the only form of phosphorous export. The extreme storm formed infiltration excess runoff to drive soil erosion and carry a large number of surface sedimentary pollutants to water body.

During the extreme storm conditions, sharp N/P enrichment would cause eutrophication and stimulate phytoplankton growth in reservoir waters, consistent with the fact that the highest cell density of algae occurred and slight cyanobacteria bloom broke out in some shallow water areas in September and October after storm events (Jia et al., 2014). In the past two decades, the concentration of total nitrogen in Miyun reservoir has increased and has approach or reached the eutrophication level (Wurtsbaugh et al., 2019; Xu et al., 2020). The first large-scale cyanobacteria bloom occurred in Miyun Reservoir in September 2002 (Wang et al., 2009). Therefore, our present findings should provide a useful reference for future research on unsteady response of eutrophication status in Miyun Reservoir to the Chaohe watershed nutrient loads. In addition, our findings suggest that high-frequency simultaneous monitoring of water quantity and quality during the whole flood season is important for reasonably estimating nutrient export and evaluating the impact of storm events on water quality, so as to consider the acceptable level of risk management for the storm size.

4.2. Effects of hydrological years on nutrient transport processes

The hydrological pulse events affected the N/P transport from the basin to the Chaohe river in terms of quality, quantity and instability. Composition and transmission pathways of nutrient export led to specific measures. However, it is unclear whether there are different nutrient transport processes in different hydrological years in semi-arid watersheds.

Runoff generation in semi-arid is complicated, including two different mechanisms, i.e., infiltration excess and saturation excess (Jiang et al., 2019). Although the rainfall amount, intensity and duration were similar between storm B and C, the streamflow and N concentration in storm B were highly variable. The sufficient rainfall in the previous stage of storm B increased the soil moisture, which was conducive to runoff generation and nutrient flush. It indicated that N transport processes were not only affected by rainfall characteristics, but also related to the overall rainfall and runoff regimes during flood season. The differences of rainfall characteristics and soil water content could cause different processes of pollution transport in semi-arid areas. The PCA and HPA results (Fig. 6a and Fig. 7a) confirmed the correlations between N variables and rainfall-runoff regime in the wet year.

Compared to 2019 storms, 2018 storms had larger concentrations and loads of all N forms; further average load exports of TN, NO_3-N, NH_4-N per event of 2018 (231, 179, 9.5 Tons) were 8-fold, 7-fold and 19-fold higher than those of 2019 (28, 25, 0.5 Tons). These results indicate the significant influence of wet years and broad discharge fluctuations in the rainy season on N dynamics. Although NO_3-N was the dominant form of N export, it accounted for a high proportion (>90 %) during flood seasons in

dry year, while <80 % in wet year. It meant that the rainfall events in the wet year caused soil erosion (Fig. S3) to increase the proportion of particulate nitrogen (PN) export and brought not only pollutants (such as chemical fertilizers and pesticides), but also a large amount of natural organic nitrogen (Org—N) into the river. PN and Org-N were delivered through surface runoff and soil water runoff have been documented in previous studies (Martin and Harrison, 2011; Inamdar et al., 2015). Thus, wet year registered complex control on N exports. Mobilization of N been different nutrient pools (surface runoff and soil water runoff) affected the N dynamics over rainy seasons in the semi-arid mountainous basin. In the dry year, seasonal patterns in subsurface runoff primarily control the N exports and composition.

Phosphorus concentration and load behaviors between dry and wet years were clearly different, which changed with discharge and different patterns existed under varied flow conditions (Table 3, Fig. 5). In wet year, P was flushed with storm runoff and PP was the dominant form, albeit in dry year, dilution of P concentrations was prominent and the storm runoff delivered the majority of TDP load (see Fig. S2). Differences in TSS exports during storms between two monitored years are the main causes for differences in P behaviors (see Fig. S3). Thus, sediment origin was important for PP exports. When rainfall events caused soil erosion, phosphorus was mainly transported and taken away in the form of sediment, resulting in the increase of PP concentration in runoff. Hence, the loss of phosphorus was dominated by PP (in wet year). When it did not cause soil erosion, it was mainly dissolved state (Figs. 4-5). Overall, erosion and sediment mobilization processes had greater control on P exports, indicating erosion contributions through surface runoff, particularly from the regions closer to the river network as the primary P export mechanism. Therefore, reducing erosion was critical for reducing nutrient transport.

Therefore, we suggest that appropriate water and soil conservation measures focusing on N/P application technology should be taken for reducing nutrient transport.

5. Conclusions

In this study, the effects of storm events on riverine nutrient dynamics in a drinking water supply river basin were initially evaluated to identify pollutant export forms and delivery processes between storm events of the two hydrological years. The results showed different pollutant forms exhibited different concentration, load, composition behaviors and transmission pathways during different storm events and hydrological years.

(1) N was mainly exported in the form of NO_3-N; while, NH_4-N registered more dynamic concentration and load behaviors between events and between different hydrological years. The dominant form of P export varied with different rainfall intensity and amount, which could be either PP or TDP.
(2) Nitrate and ammonium had different supply sources and transport mechanisms. While NH_4-N was mainly washed via surface runoff from over-land sources, NO_3-N and TN were mostly delivered via subsurface runoff. TP was primarily associated with overland sources and transported by surface runoff.
(3) Rainfall characteristics (i.e. intensity, amount) had significant control over P dynamics. The extreme storm event often registered the highest nutrient concentrations and largest pollutant load exports. It especially played a key role in TP exports, accounting for 94 % of the total TP load exports.
(4) N dynamics displayed stronger correlations with hydrological processes (i.e., rainfall, discharge) than individual rainfall features. N dynamics through two years suggested complex control on TN exports by both soil water runoff and surface runoff associated sources in the wet year. Storm events of the wet year often registered the higher N concentration and more pollutant load exports, which might lead to the greater risk of eutrophication. Dominant forms of P were inconsistent between two hydrological years. PP was the dominant P form in wet years, but TDP in dry year.

These findings allowed us to gain a comprehensive understanding of the nutrient export process and export controls during the rainy season in a drinking water source basin. And it could be served as a reference for establishing water quality monitoring programs and determining effective pollution mitigation strategies in the future.

CRediT authorship contribution statement

Yan Jiang: Conceptualization, Methodology, Investigation, Formal analysis, Writing - original draft, Funding acquisition.
Xin Bao: Investigation, Data curation, Visualization.
Zhengfang Huang: Resources, Data support.
Yiping Chen: Investigation, Visualization.
Xianing Wu: Writing - review & editing.
Xuyong Li: Resources, Supervision, Funding acquisition.
Xuefeng Wu: Visualization.
Yucong Hu: Investigation, English polishing, Spell checking, Proofreading.

Data availability

Data will be made available on request.

Declaration of competing interest

The authors declare that they have no known competing financial interests or personal relationships that could have appeared to influence the work reported in this paper.

Acknowledgements

This work was supported by the National Key Research and Development Program of China (No. 2019YFB2102902). The author are grateful to Dr. H.K.M. Mihiranga and Dr. Chen Cao for their assistances in PCA analysis, to the anonymous reviewers for their valuable comments and suggestions.

Appendix A. Supplementary data

Supplementary data to this article can be found online at https://doi.org/10.1016/j.scitotenv.2023.163606.

References

Adyel, T.M., Oldham, C.E., Hipsey, M.R., 2017. Storm event-scale nutrient attenuation in constructed wetlands experiencing a Mediterranean climate: a comparison of a surface flow and hybrid surface-subsurface flow system. Sci. Total Environ. 598, 1001–1014. https://doi.org/10.1016/j.scitotenv.2017.04.044.

Aguilera, R., Melack, J.M., 2018. Concentration-discharge responses to storm events in coastal California watersheds. Water Resour. Res. 54, 407–424. https://doi.org/10.1002/2017WR021578.

Alvarez-Cobelas, M., Angeler, D.G., Sanchez-Carrillo, S., 2008. Export of nitrogen from catchments: a worldwide analysis. Environ. Pollut. 156 (2), 261–269. https://doi.org/10.1016/j.envpol.2008.02.016.

Austin, A.T., Yahdjian, L., Stark, J.M., Belnap, J., Porporato, A., Norton, U., Ravetta, D.A., Schaeffer, S.M., 2004. Water pulse and biogeochemical cycles in arid and semiarid ecosystems. Oecologia 141, 221–235. https://doi.org/10.1007/s00442-004-1519-1.

Ballantine, D.J., Walling, D.E., Collins, A.L., Leeks, G.J.L., 2006. Phosphorus storage in fine channel bed sediments. Water Air Soil Pollut. Focus 6, 371–380. https://doi.org/10.1007/s11267-006-9029-2.

Ballantine, D.J., Walling, D.E., Collins, A.L., Leeks, G.J.L., 2008. The phosphorus content of fluvial suspended sediment in three lowland groundwater-dominated catchments. J. Hydrol. 357, 140–151. https://doi.org/10.1016/j.jhydrol.2008.05.011.

Bender, M.A., dos Santos, D.R., Tiecher, T., et al., 2018. Phosphorus dynamics during storm events in a subtropical rural catchment in southern Brazil. Agric. Ecosyst. Environ. 261, 93–102. https://doi.org/10.1016/j.agee.2018.04.0,04.

Blaen, P.J., Khamis, K., Lloyd, C., Comer-Warner, S., Ciocca, F., Thomas, R.M., MacKenzie, A.R., Krause, S., 2017. High-frequency monitoring of catchment nutrient exports reveals highly variable storm event responses and dynamic source zone activation. 2017. J. Geophys. Res. Biogeosci. 122, 2265–2281. https://doi.org/10.1002/2017JG003904.

Bowes, M.J., House, W.A., Hodgkinson, R.A., Leach, D.V., 2005. Phosphorus-discharge hysteresis during storm events along a river catchment: the river swale, UK. Water Res. 39, 751–762. https://doi.org/10.1016/j.watres.2004.11.027.

Bowes, M.J., Jarvie, H.P., Halliday, S.J., et al., 2015. Characterising phosphorus and nitrate inputs to a rural river using high-frequency concentration-flow relationships. Sci. Total Environ. 511, 608–620. https://doi.org/10.1016/j.scitotenv.2014.12.086.

Burrus, D., Thomas, R.L., Dominik, B., Vernet, J.-P., Dominik, J., 1990. Characteristics of suspended sediment in the upper Rhone River, Switzerland, including the particulate forms of phosphorus. Hydrol. Process. 4, 85–98.

Chen, N.W., Wu, J.Z., Hong, H.S., 2012. Effect of storm events on riverine nitrogen dynamics in a subtropical watershed, southeastern China. Sci. Total Environ. 431, 357–365. https://doi.org/10.1016/j.scitotenv.2012.05.072.

Correll, D.L., Jordan, T.E., Weller, D.E., 1999. Transport of nitrogen and phosphorus from Rhode River watersheds during storm events. Water Resour. Res. 35 (8), 2513–2521. https://doi.org/10.1029/1999wr900058.

Cui, Z.L., Zhang, H.Y., Chen, X.P., Zhang, C.C., Ma, W.Q., Huang, C.D., Zhang, W.F., Mi, G.H., Miao, Y.X., Li, X.L., Gao, Q., Yang, J.C., Wang, Z.H., Ye, Y.L., Guo, S.W., Lu, J.W., Huang, J.L., Lv, S.H., Sun, Y.X., Liu, Y.Y., Peng, X.L., Ren, J., Li, S.Q., Deng, X.P., Shi, X.J., Zhang, Q., Yang, Z.P., Tang, L., Wei, C.Z., Jia, L.L., Zhang, J.W., He, M.G., Tong, Y.N., Tang, Q.Y., Zhong, X.H., Liu, Z.H., Cao, N., Kou, C.L., Ying, H., Yin, Y.L., Jiao, X.Q., Zhang, Q.S., Fan, M.S., Jiang, R.F., Zhang, F.S., Dou, Z.X., 2018. Pursuing sustainable productivity with millions of smallholder farmers. Nature 555 (7696), 363–366.

Guo, C.F., Zhi, D., Guo, X.Y., 2021. Spatial and temporal analysis of water quality from 1991 to 2011 in miyun reservoir. Environ. Geochem. Health 43, 4395–4413. https://doi.org/10.1007/s10653-021-00928-9.

Hinckley, B.R., Etheridge, J.R., Peralta, A.L., 2019. Storm event nitrogen dynamics in waterfowl impoundments. Water Air Soil Pollut. 230, 294. https://doi.org/10.1007/s11270-019-4332-5.

Inamdar, S., Dhillon, G., Singh, S., Parr, T., Qin, Z., 2015. Particulate nitrogen exports in stream runoff exceed dissolved nitrogen forms during large tropical storms in a temperate, headwater, forested watershed. J. Geophys. Res. G: Biogeosci. 120, 1548–1566. https://doi.org/10.1002/2015JG002909.

Janke, B.D., Finlay, J.C., Hobbie, S.E., Bake, L.A., Sterner, R.W., Nidzgorski, D., Wilson, B.N., 2014. Contrasting influences of stormflow and baseflow pathways on nitrogen and phosphorus export from an urban watershed. Biogeochemistry 121 (1), 209–228. https://doi.org/10.1007/s10533-013-9926-1.

Jarvie, H.P., Sharpley, A.N., Scott, J.T., 2012. In the watershed phosphorus puzzle. Environ. Sci. Technol. 46, 13284–13292.

Jia, D.M., Wang, J.S., Wang, C.G., 2014. Practice and thinking of water bloom prevention and control in miyun reservoir. Beijing Water 5, 19–22 (in Chinese).

Jiang, Y., Liu, C.M., Li, X.Y., Liu, L.F., Wang, H.R., 2015. Rainfall-runoff modeling, parameter estimation and sensitivity analysis in a semiarid catchment. Environ. Model. Softw. 67, 72–88. https://doi.org/10.1016/j.envsoft.2015.01.008.

Jiang, Y., Liu, C.M., Hao, S.N., Zhao, H.T., Li, X.Y., 2019. A framework to develop a watershed pollution load model for semiarid and semihumid areas. J. Hydrol. 579, 124179. https://doi.org/10.1016/j.jhydrol.2019.124179.

Kämäri, M., Tattari, S., Lotsari, E., Koskiaho, J., Lloyd, C.E.M., 2018. High-frequency monitoring reveals seasonal and event-scalewater quality variation in a temporally frozen river. J. Hydrol. 564, 619–639. https://doi.org/10.1016/j.jhydrol.2018.07.037.

Kelly, P.T., Renwick, W.H., Knoll, L., 2019. Stream nitrogen and phosphorus loads are differentially affected by storm events and the difference may be exacerbated by conservation tillage. Environ. Sci. Technol. 53, 5613–5621. https://doi.org/10.1021/acs.est.8b05152.

Li, R.N., Zheng, H., O'Connor, P., Xu, H.S., Li, Y.K., Lu, F., Robinson, B.E., Ouyang, Z.Y., Hai, Y., Daily, G.C., 2021. Time and space catch up with restoration programs that ignore ecosystem service trade-offs. Sci. Adv. 7, eabf8650. https://doi.org/10.1126/sciadv.abf8650.

Li, X.Y., Meixner, T., Sickman, J.O., Miller, A.E., Schimel, J.P., Melack, J.M., 2006. Decadal-scale dynamics of water, carbon and nitrogen in a California chaparral ecosystem: DAYCENT modeling results. Biogeochemistry 77, 217–245. https://doi.org/10.1007/s10533-005-1391-z.

Lloyd, C.E.M., Freer, J.E., Johnes, P.J., Collins, A.L., 2016. Using hysteresis analysis of high resolution water quality monitoring data, including uncertainty, to infer controls on nutrient and sediment transfer in catchments. Sci. Total Environ. 543, 388–404. https://doi.org/10.1016/j.scitotenv.2015.11.028.

Ma, X., Li, Y., Li, B.L., Han, W.Y., Liu, D.B., Gan, X.Z., 2016. Nitrogen and phosphorus losses by runoff erosion: field data monitored under natural rainfall in three gorges reservoir area, China. Catena 147, 797–808. https://doi.org/10.1016/j.catena.2016.09.004.

Macrae, M.L., English, M.C., Schiff, S.L., Ston M., e., 2010. Influence of antecedent hydrologic conditions on patterns of hydrochemical export from a first-order agricultural watershed in Southern Ontario, Canada. J. Hydrol. 389, 101–110. https://doi.org/10.1016/j.jhydrol.2010.05.034.

Martin, R.A., Harrison, J.A., 2011. Effect of high flow events on in-stream dissolved organic nitrogen concentration. Ecosystems 14, 1328–1338. https://doi.org/10.1007/s10021-011-9483-1.

Mihiranga, H.K.M., Jiang, Y., Li, X.Y., Wang, W., De Silva, K., Kumwimba, M.N., Bao, X., Nissanka, S.P., 2021. Nitrogen/phosphorus behavior traits and implications during storm events in a semi-arid mountainous watershed. Sci. Total Environ. 791, 148382. https://doi.org/10.1016/j.scitotenv.2021.148382.

Mihiranga, H.K.M., Jiang, Y., Sathsarani, M.G.S., Li, X.Y., Wang, W., 2022. Identification of rainy season nitrogen export controls in a semi-arid mountainous watershed, North China. Sci. Total Environ. 839, 156293. https://doi.org/10.1016/j.scitotenv.2022.156293.

Nguyen, H., Meon, G., Nguyen, V., 2019. Development of an event-based water quality model for sparsely gauged catchments. Sustainability 11, 1773. https://doi.org/10.3390/su11061773.

Owens, L.B., Shipitalo, M.J., Bonta, J.V., 2008. Water quality response times to pasture management changes in small and large watersheds. J. Soil Water Conserv. 63 (5), 292–299. https://doi.org/10.2489/jswc.63.5.292.

Pionke, H.B., Gburek, W.J., Schnabel, R.R., Sharpley, A.N., Elwinger, G.F., 1999. Seasonal flow, nutrient concentrations and loading patterns in stream flow draining an agricultural hill-land watershed. J. Hydrol. 220 (1–2), 62–73. https://doi.org/10.1016/s0022-1694(99)00064-5.

Quan, N.H., Meon, G., 2015. Nutrient dynamics during flood events in tropical catchments: a case study in Southern Vietnam. Clean: Soil, Air, Water 43 (5), 621–786. https://doi.org/10.1002/clen.201300264 2015.

R Core Development Team, 2008. R: a language and environment for statistical computing. http://www.R-project.org/.

Royer, T.V., David, M.B., Gentry, L.E., 2006. Timing of riverine export of nitrate and phosphorus from agricultural watersheds in Illinois: implications for reducing nutrient loading to the Mississippi River. Environ. Sci. Technol. 40 (13), 4126–4131. https://doi.org/10.1021/es052573n.

Schilling, K., Zhang, Y.K., 2004. Baseflow contribution to nitrate-nitrogen export from a large, agricultural watershed, USA. J. Hydrol. 295 (1-4), 305–316. https://doi.org/10.1016/j.jhydrol.2004.03.010.

Wagne, L.E., Vidon, P., Tedesco, L.P., Gray, M., 2008. Stream nitrate and DOC dynamics during three spring storms across land uses in glaciated landscapes of the Midwest. J. Hydrol. 362, 177–190. https://doi.org/10.1016/j.jhydrol.2008.08.013.

Walling, D.E., Owens, P.N., Carter, J., et al., 2003. Storage of sediment-associated nutrients and contaminants in river channel and floodplain systems. Appl. Geochem. 18, 195–220. https://doi.org/10.1016/S0883-2927(02)00121-X.

Wang, Q.S., Mei, X.R., Zhang, Y.Q., Sun, D.B., Yu, Y.L., 2009. Review of water quality of miyun reservoir. J. Agric. Sci. Technol. 11 (1), 45–50 (In Chinese).

Wang, X.M., Zhang, X., Hasi, E., Dong, Z.B., 2010. Has the three norths Forest shelterbelt program solved the desertification and dust storm problems in arid and semiarid China? J. Arid Environ. 74 (1), 13–22. https://doi.org/10.1016/j.jaridenv.2009.08.001.

Wang, X.Y., Li, Z.Q., Li, M.T., 2018. Impacts of climate change on stream flow and water quality in a drinking water source area, Northern China. Environ. Earth Sci. 77, 410. https://doi.org/10.1007/s12665-018-7581-5.

Williams, M.R., Livingston, S.J., Penn, C.J., Smith, D.R., King, K.W., Huang, C.H., 2018. Controls of event-based nutrient transport within nested headwater agricultural watersheds of the western Lake Erie basin. J. Hydrol. 559, 749–761. https://doi.org/10.1016/j.jhydrol.2018.02.079.

Williamson, T.J., Vanni, M.J., Renwick, W.H., 2020. Spatial and temporal variability of nutrient dynamics and ecosystem metabolism in a hyper-eutrophic reservoir differ between a wet and dry year. Ecosystems 24, 68–88. https://doi.org/10.1007/s10021-020-00505-8.

Wurtsbaugh, W.A., Paerl, H.W., Dodds, W.K., 2019. Nutrients, eutrophication and harmful algal blooms along the freshwater to marine continuum. Wires. Water 6 (5), 1–27. https://doi.org/10.1002/wat2.1373.

Xu, R.H., Cai, Y.P., Wang, X., Li, C.H., Liu, Q., Yang, Z.F., 2020. Agricultural nitrogen flow in a reservoir watershed and its implications for water pollution mitigation. J. Clean. Prod. 267, 122034. https://doi.org/10.1016/j.jclepro.2020.122034.

Zhang, J., Qiao, R.R., Song, Y.Y., Lai, Y.Q., 2022. Assessing runoff and pollutant loading upstream of the miyun reservoir for sustainable water resources management. Water Environ. J. 2022 (36), 115–131. https://doi.org/10.1111/wej.12748.

Zhang, Q.F., Wu, Z.F., Guo, G.H., Zhang, H., Tarolli, P., 2020. Explicit the urban waterlogging spatial variation and its driving factors: the stepwise cluster analysis model and hierarchical partitioning analysis approach. Sci. Total Environ. 763 (2021), 143041. https://doi.org/10.1016/j.scitotenv.2020.143041.

Zhao, G., Li, M.S., 1991. Preliminary benefits have been made in the key prevention work for soil and water conservation in the upper reaches of miyun reservior. Soil Water Conserv. China 112 (8), 14–16 (In chinese).

Zheng, H., Robinson, B.E., Liang, Y.C., Polasky, S., Ma, D.C., Wang, F.C., Ruckelshaus, M., Ouyang, Z.Y., Daily, G.C., 2013. Benefits, costs, and livelihood implications of a regional payment for ecosystem service program. Proc. Natl. Acad. Sci. U. S. A. 110 (41), 16681–16686.

Zhou, Y., Zhang, Y.L., Abbaspour, K.C., Mosler, H.J., Yang, H., 2009. Economic impacts on farm households due to water reallocation in China's chaobai watershed. Agr. Water Manage. 96 (5), 883–891. https://doi.org/10.1016/j.agwat.2008.11.011.